Materials Characterization 176 (2021) 111112

Contents lists available at ScienceDirect

Materials Characterization

journal homepage: www.elsevier.com/locate/matchar

Simultaneously enhancing strength and ductility of Ti-6Al-4V alloy with the hierarchical structure via a novel thermal annealing treatment

Le Wang [a,b], Hao Ma [b], Qunbo Fan [a,b,*], Jiahao Yao [a], Xinyu Shen [b], Shiyi Zhang [b], Yu Zhou [a], Yi Peng [a], Yu Gao [a,b], Duoduo Wang [a,b]

[a] Beijing Institute of Technology Chongqing Innovation Center, Chongqing 401135, China
[b] School of Materials Science and Engineering, Beijing Institute of Technology, Beijing 100081, China

ARTICLE INFO

Keywords:
Ti-6Al-4V
Spark plasma sintering
Mechanical properties
Solution and aging

ABSTRACT

A novel solution and aging (STA) heat treatment was proposed to improve the strength and ductility of Ti-6Al-4V alloy simultaneously. Effects of the novel heat treatment on microstructure and mechanical properties of the Ti-6Al-4V alloy prepared by spark plasma sintering (SPS) were studied in this work. The crystalline structure and microstructure of both the as-fabricated Ti-6Al-4V alloy and the STA Ti-6Al-4V alloy were observed using X-ray diffraction (XRD) technique, optical microscope (OM), scanning electron microscopy (SEM), and transmission electron microscopy (TEM), respectively. The XRD patterns indicated that the two Ti-6Al-4V samples have the similar crystalline structure with α phase and β phase. However, the results of OM images suggested that the microstructure of Ti-6Al-4V alloy was transformed from the Widmanstätten structure to a hierarchical structure which included the basket-weave structure and the Widmanstätten structure after the STA heat treatment. Apart from the above-mentioned microstructure, the hierarchical structure also exhibited specifically some fine dispersed β surrounded by some equiaxed α. Moreover, the results of the room temperature tensile tests revealed that the STA heat treatment could improve the strength and ductility of the Ti-6Al-4V alloy simultaneously. Based on the observation of TEM images, the increment of the elongation of the STA Ti-6Al-4V alloy can be attributed to the effect of annealing twins and equiaxed α, and the total strength increments should be caused by the dispersion strengthening effect of the dispersed β.

1. Introduction

Titanium and its alloys are widely used in aerospace, medical implant, military, and energy industries due to their good corrosion resistance, high specific strength, and good biocompatibility [1,2]. Among these titanium alloys, the Ti-6Al-4V alloy is known as the workhorse of the titanium industry because it possesses a favorable combination of strength and ductility [3,4]. However, with the continuous development of the industry, the strength and ductility of the present Ti-6Al-4V alloy can't gradually meet the performance requirements for the new special materials, resulting in the limitation of the application of Ti-6Al-4V alloy. Therefore, the study on improving the mechanical properties of Ti-6Al-4V alloy has attracted more attention.

Ti-6Al-4V alloy is the typical (α + β) two-phase titanium alloy, which is composed of hexagonal close-packed (HCP) α phase and body-centered cubic (BCC) β phase. Generally, Ti-6Al-4V alloy has four kinds of typical microstructure, i.e., fully lamellar, bi-modal, equiaxed, and basket-weave microstructure. As it is well known, the mechanical properties of titanium alloy strongly depend on its microstructure which can be controlled by thermo-mechanical treatments [5,6]. Meanwhile, for Ti-6Al-4V alloy, the morphology, fraction, size, and distribution of various phases can significantly influence its mechanical properties [7]. Therefore, the improvement of the strength and ductility of the Ti-6Al-4V alloy can be expected to achieve by a thermo-mechanical treatment.

Up to now, some scientists have made efforts to improve the mechanical properties of Ti-6Al-4V alloy by some thermo-mechanical treatments. For example, Chong et al. [8,9] obtained the bi-lamellar microstructure with both high tensile strength and large ductility in Ti-6Al-4V alloy by the intercritical annealing treatments. They found that compared with that of the lamellar microstructure, the yield strength of the bi-lamellar microstructure could be significantly enhanced. Especially for the bi-lamellar microstructure with the colony size of 60 μm, the ultimate strength was 1100 MPa and the total elongation was 18.6%, which is significantly higher than that of full lamellar

* Corresponding author at: Beijing Institute of Technology Chongqing Innovation Center, Chongqing 401135, China.
E-mail address: fanqunbo@bit.edu.cn (Q. Fan).

https://doi.org/10.1016/j.matchar.2021.111112
Received 24 February 2021; Received in revised form 6 April 2021; Accepted 7 April 2021
Available online 15 April 2021

microstructure. Cao et al. [10] fabricated Ti-6Al-4V alloy with a finer prior-β grain size by vacuum sintering at the β-transus (1010 °C) temperature, which showed that Ti-6Al-4V alloy can have a tensile strength of ~1130 MPa and elongation of ~10% by hydrogenation-dehydrogenation treatment. Moreover, Jia et al. [11] reported a Ti-6Al-4V alloy with a relatively high oxygen content of 0.52 wt%, which had a very high ultimate tensile strength of 1421.7 MPa and an elongation to fracture of 7.2%. It is worth noting that some subsequent hot deformations were examined during the above thermo-mechanical treatments, which were complicated and difficult to control, and needed higher costs, though the optimization of mechanical properties of Ti-6Al-4V alloy can be obtained. Moreover, for most of the heat treatments without the deformation, they generally optimized the mechanical properties of Ti-6Al-4V alloy by adjusting the proportion, size, or distribution of α phase and β phase in the alloy during the annealing process [7]. Unfortunately, these conventional heat treatments usually cannot achieve the simultaneous increase of strength and ductility of Ti-6Al-4V alloy. Recently, some studies have found that the hierarchical structure can circumvent the strength-ductility trade-off for Ti alloy [12,13]. Kang et al. [12] had used a methodology of powder sintering and in-situ press forging to a novel hierarchical microstructure in Ti-6Al-4V alloy. The hierarchical microstructure, which contains the typical triangle colonies with ultrafine lamellar α and β, and their border areas with ultrafine equiaxed α, dispersed nano/ultrafine β, as well as α/β interface L layers, was called as bimorphic microstructure in their work. In their work, the Ti-6Al-4V alloy with the special microstructure exhibited a high tensile ultimate strength of 1240 ± 20 MPa and fracture elongation of 19.5 ± 35 MPa. Moreover, A. Devaraj et al. [13] used a methodology of powder sintering and hot rod-rolling followed by the solid solution treatment of 1450 °F for 1 h and 900 °F for 2 h to prepare the Ti-1Al-8V-5Fe alloy with a hierarchical nanostructure consisting of a homogenous distribution of micron-scale and nanoscale α-phase precipitates within the β-phase matrix. The ultimate tensile strength value was up to 1690 MPa, which is higher than that of most Ti alloys. In this case, the elongation was still up to 5%. This suggested that the mechanical properties of the Ti-1Al-8V-5Fe alloy with hierarchical nanostructure were excellent. Nevertheless, it is found that few studies are made to design the hierarchical structure by a simple heat treatment to improve the strength and ductility of Ti-6Al-4V alloy. Therefore, a novel hierarchical microstructure was intended to be formed by the simple heat treatment without hot deformation to simultaneously improve the strength and ductility of Ti-6Al-4V alloy in our study, which would be necessary and beneficial for the industrial application. Moreover, spark plasma sintering (SPS) has been developed to be a novel method of powder metallurgy, which has the advantages of a short time, low temperature, and high density [14]. More importantly, SPS can be used to fabricate the small sample, which can save the cost for studying the effect of the heat treatment on microstructure and mechanical properties of Ti alloy.

In this work, the Ti-6Al-4V alloy was prepared by SPS. Thermal annealing treatment for the as-fabricated Ti-6Al-4V alloy was carried out to obtain a novel microstructure, which can simultaneously enhance the strength and ductility of the Ti-6Al-4V alloy. The crystalline structure, microstructural evolution, and mechanical properties of Ti-6Al-4V alloy with a novel microstructure were investigated to reveal the detailed mechanism of performance optimization.

2. Experiments

The raw materials were the commercially gas atomized Ti-6Al-4V powders with the range of 53–106 μm in particle size (as shown in Fig. 1). These Ti-6Al-4V powders were produced by falcontech col., Ltd. The corresponding chemical composition was listed in Table 1. These Ti-6Al-4V powders (about 30 g) were put in a graphite die (outside diameter, 45 mm; inside diameter, 30 mm; height, 40 mm). The graphite die filled with Ti-6Al-4V powers was placed into the cavity of an SPS equipment (FTC Group, SE-607, Germany) and then were heated up to 900 °C in an argon atmosphere at a heating rate of about 100 °C/min. During the sintering process, the pressure was held at 50 MPa and the hold time was 5 min. As Fig. 1 shows, two Ti-6Al-4V samples were prepared under the above same sintering condition in our work. One of the two Ti-6Al-4V samples was solution treated at 1050 °C for 30 min, water quenched and aged at 900 °C for 2 h, furnace cooled, and this sample is called STA Ti-6Al-4V sample. For the other Ti-6Al-4V sample prepared by SPS, no heat treatment was carried out, and this sample is called the as-fabricated Ti-6Al-4V sample. The flow diagram of detailed processes is shown in Fig. 2.

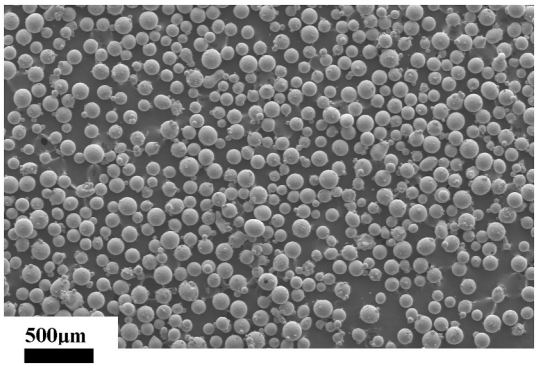

Fig. 1. The surface morphology of origin Ti-6Al-4V powders.

Table. 1
The chemical composition of origin Ti-6Al-4V powders.

Element	Ti	Al	V	Fe	C	O	N	H
wt%	Bal.	6.3	4.3	0.1	0.06	0.10	0.02	0.001

The crystal structure of the as-fabricated Ti-6Al-4V sample and the STA Ti-6Al-4V sample was confirmed by X-ray diffraction (XRD, Philips X'pert PRO) with Cu Kα radiation (Wavelength: 0.15418 nm). The microstructural characteristics of the samples were investigated by optical microscope (OM, ZEISS AxioCam MRC 5), scanning electron microscope (SEM, FEI Sirion 200), and transmission electron microscopy (TEM, Tecnai TF20 TMP). The dog-bone-shaped specimens (16 × 4 × 0.75 mm^3) were cut from the two kinds of Ti-6Al-4V samples using the electrical discharge machining technique and tested using an INSTRON-5581 universal testing machine with a rate of 0.3 mm/s at room temperature. To reduce the effects of the scratches and other defects on the tensile test results, all the tensile samples were mechanically polished with 80–2000 grid SiC paper before testing. For each condition, at least

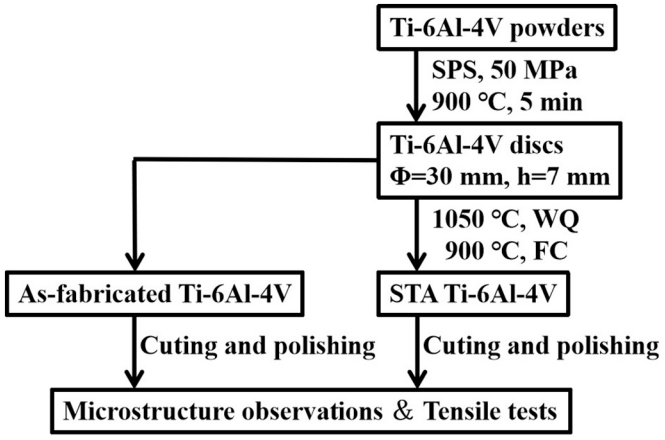

Fig. 2. A sketch of working processes.

three specimens were tensile tested and the typical stress-strain curve, which was highly reproducible, was selected to exhibit the tensile properties. The extensometer was used to measure the strain.

3. Results and discussion

3.1. Crystalline structure of as-fabricated Ti-6Al-4V sample and STA Ti-6Al-4V sample

To study the effect of the heat treatment on the crystalline structure of Ti-6Al-4V alloy, the XRD patterns of the as-fabricated Ti-6Al-4V sample and the STA Ti-6Al-4V sample were shown in Fig. 3, respectively. The results of Fig. 3 suggest that both as-fabricated Ti-6Al-4V sample and STA Ti-6Al-4V sample are composed of α phase and β phase. The intensity of α (101) is the highest among these peaks. Meanwhile, it is noted that the intensity of some α phase peaks in the Ti-6Al-4V alloy becomes low and the intensity of β phase peak does not seem to change after the solution and aging treatment. As shown in Fig. 3, the intensity of α (100), α (110), and α (103) in the STA Ti-6Al-4V sample is lower than that in the as-fabricated Ti-6Al-4V sample. This is because the content of some α phases increased and the content of some other α phases decreased after the solution and aging treatment. This indicates that the texture of the α phase is affected during the heat treatment process . The intensity of the β phase was very low, which indicated that the volume fraction of the β phases in the two Ti-6Al-4V samples was very small. Although the intensity of some phases in the two Ti-6Al-4V samples has a little difference, the crystalline structure is still similar.

3.2. Microstructure characterization of as-fabricated Ti-6Al-4V sample and STA Ti-6Al-4V sample

The representative optical micrographs (OMs) and SEM images of the as-fabricated Ti-6Al-4V sample and the STA Ti-6Al-4V sample are presented in Fig. 4, respectively. As shown in Fig. 4(a), the as-fabricated Ti-6Al-4V alloy has a typical Widmanstätten structure, consisting of grain boundary α (called as α_{GB}) located at β grain boundaries and α colonies within β matrix. For the Widmanstätten structure, it was formed during the sintering process. As is reported, the Widmanstätten structure can be formed in the $\beta \rightarrow \alpha + \beta$ transformation process upon the slow cooling at the specific temperature [15–17]. Besides, the β grain size of the as-fabricated Ti-6Al-4V sample was calculated to be 117 ± 40 μm by counting more than about 300 β grains in many OMs (more than tens of OMs). For the STA Ti-6Al-4V sample, as shown in Fig. 4(b), the size of β

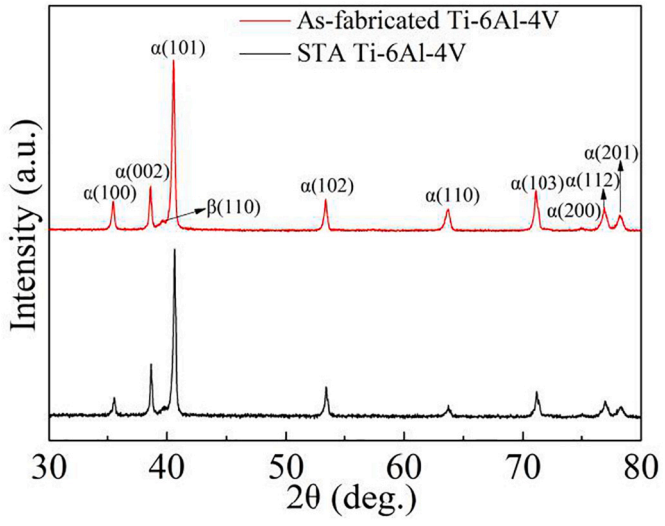

Fig. 3. XRD patterns of as-fabricated Ti-6Al-4V sample and STA Ti-6Al-4V sample.

grains was 126 ± 20 μm, which have almost no significant increase compared with that of the as-fabricated Ti-6Al-4V sample. This indicates that the influences of the STA heat treatment on the grain size of β grain are negligible. Meanwhile, it is easily seen that the microstructure of the STA Ti-6Al-4V sample had made a great change after the heating treatment process. As shown in Fig. 4(b), it is noted that apart from the Widmanstätten microstructure and basket-weave microstructure, some fine β phases surrounded by many equiaxed phases were also found in the STA Ti-6Al-4V sample, which is consistent with the results of A. Safdar et al. [18]. The formation process of the special structure (called as the hierarchical structure) can be divided into two stages. During the solution and water quenching treatment, the rapid cooling in β phase region (1050 °C, WQ) resulted in the formation of basket-weave microstructure with α' martensite. Moreover, some residual β phases might also exist alongside α' martensite. Then, during the following aging stage (900 °C, FC), α' martensite would transform to α + β microstructure. Meanwhile, the residual β phase also transformed to α + β phase [19,20]. After the above two transformations, the fine β phases and equiaxed α phases would be formed. The size range of these fine β phases was from several microns to hundreds of nanometers. Furthermore, there was still the basket-weave microstructure in the STA Ti-6Al-4V sample. It is because some of the basket-weave microstructure formed after 1050 °C WQ was retained during the aging treatment. Moreover, the α_{GB} in the Ti-6Al-4V alloy became fine but didn't disappear after the 1050 °C WQ treatment. Thus, some α colonies would be reproduced from the α_{GB}/β interfaces to form the Widmanstätten structure marked by the red arrow in Fig. 4(b). To further distinguish the difference of microstructure between the as-fabricated Ti-6Al-4V sample and the STA Ti-6Al-4V sample, the typical SEM image of higher magnification was shown in Fig. 4(c) and Fig. 4(d). Based on the above discussion, the forming reasons of the mixed morphology in the STA Ti-6Al-4V sample could be obtained. Specifically, the formation schematic of the Ti-6Al-4V sample with a hierarchical structure was shown in Fig. 5. As for the effects of the microstructural characteristic on the mechanical properties of the Ti-6Al-4V sample, it will be discussed in a subsequent section.

3.3. Comparison of tensile properties of Ti-6Al-4V sample and STA Ti-6Al-4V sample

Tensile stress-strain curves of the as-fabricated Ti-6Al-4V sample and the STA Ti-6Al-4V sample at room temperature are shown in Fig. 6 to indicate the effect of the STA heat treatment on the tensile properties of Ti-6Al-4V alloy. As shown in Fig. 6, the yield strength (YS) and the ultimate tensile strength (UTS) of the STA Ti-6Al-4V sample are 790 MPa and ultimate tensile strength (UTS) of 893 MPa, respectively, which is 80 MPa and 49 MPa more than that of the as-fabricated Ti-6Al-4V sample. Meanwhile, the elongation value of the Ti-6Al-4V alloy increased from 12% to 16.8% through the STA heat treatment process. The above results suggest that the strength and ductility of the Ti-6Al-4V were enhanced simultaneously by the STA heat treatment. The results of tensile properties should be closely related to the microstructure of the Ti-6Al-4V alloy. To illustrate the effect of the STA heat treatment on the tensile properties of the Ti-6Al-4V alloy, fracture surface morphologies, and TEM observations of the Ti-6Al-4V alloy will be discussed next.

3.4. Fracture surface morphologies

Fig. 7 shows the tensile fractography of the as-fabricated Ti-6Al-4V sample and the STA Ti-6Al-4V sample. As shown in Fig. 7(a), the as-fabricated Ti-6Al-4V sample mainly had a mixed fracture morphology of both brittle cleavage fracture with cleavage surface and ductile fracture with shallow dimples. The river patterns marked by the red arrow with numerous shallow and parallel tearing ridges were also observed in the fracture surface of the as-fabricated Ti-6Al-4V sample. Berg et al. [21] and Cao et al. [22] claimed that these cleavage surfaces

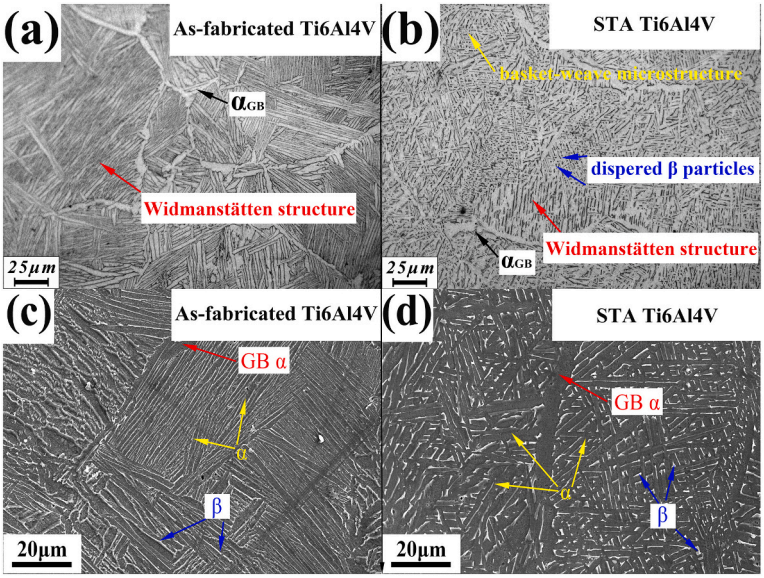

Fig. 4. Optical micrographs and SEM images of (a) and (c) as-fabricated Ti-6Al-4V sample, and (b) and (d) STA Ti-6Al-4V sample.

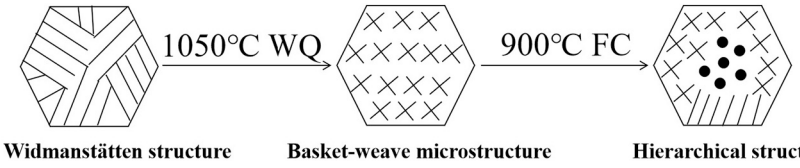

Fig. 5. Formation schematic of Ti-6Al-4V sample with a hierarchical structure.

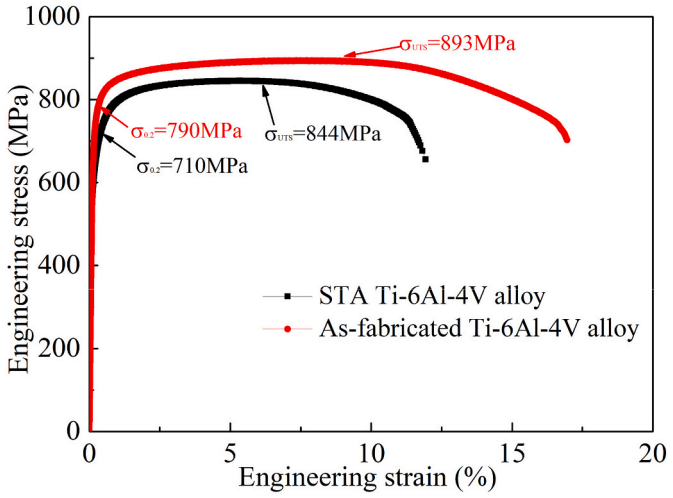

Fig. 6. Engineering stress-strain curves of as-fabricated Ti-6Al-4V sample and STA Ti-6Al-4V sample.

should be caused by the fracture of the continuous α_{GB} layers which were also observed by the optical microscope and SEM. Though some dimples also existed in the fracture surface of the as-fabricated Ti-6Al-4V sample, these dimples were very shallow and the number of these dimples was not great. On the contrary, the fracture morphology of the STA Ti-6Al-4V sample with a ductile fracture mode is shown in Fig. 7(b). There were a large number of dimples (marked by blue arrows) in the fracture surface of the STA Ti-6Al-4V sample. These dimples were deeper than that of the as-fabricated Ti-6Al-4V sample. This also demonstrates that the Ti-6Al-4V sample by the STA heat treatment has higher ductility, which was in agreement with the results of the tensile tests.

3.5. TEM analysis

To confirm the cause of the simultaneous improvement of strength and ductility of the Ti-6Al-4V alloy, TEM images of the STA Ti-6Al-4V sample are presented in Fig. 8. As shown in Fig. 8(a), some twins were found at the α/β interface, which can be formed during the STA heat treatment. The formation of annealing twins could result from the low stacking fault energy of the Ti-6Al-4V alloy. As claimed by Deng et al. [23], the existence of these annealing twins can provide adequate strain hardening to delay necking and ensure a combination of high strength and reasonable plasticity. Therefore, these annealing twins present in the STA Ti-6Al-4V sample can be beneficial for increasing ductility. Meanwhile, as shown in Fig. 8(b), surprisingly, there are some fine particles in the grain interiors, which is in accord with the results of Fig. 4(b) and Fig. 4(d). The selected area electron diffraction patterns shown in Fig. 8(c-d) confirmed that these finely dispersed phases and the ambient equiaxed phases were corresponding to the diffraction spots of the β phase and the α phase, respectively. These equiaxed α phases should be formed during the furnace cooling process. Fig. 8(e) exhibits the region of energy dispersive spectroscopy (EDS), in which the β phase were embedded in the equiaxed α phase. As shown in Fig. 8(f) and Fig. 8 (g), large amounts of V element (β stabilizer) are detected in the β phases, and the composition of V is higher than that in the equiaxed α phases. While Al as the α stabilizer was enriched in the α phase, and the composition of Al is higher than that in the β phase. The phenomenon was found by Safdar et al. [18]. The results of element distribution (Al and V) indicated that the formation of the α + β structure should be caused by the diffusion-controlled transformation in which large numbers of V diffused to the β phase while Al diffused to the α phase. As reported by Kang et al. [12], the equiaxed structure can also contribute

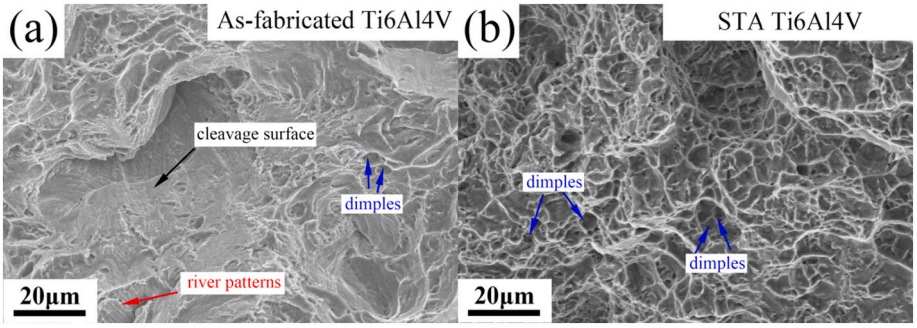

Fig. 7. Fracture surfaces of (a) as-fabricated Ti-6Al-4V sample and (b) STA Ti-6Al-4V sample.

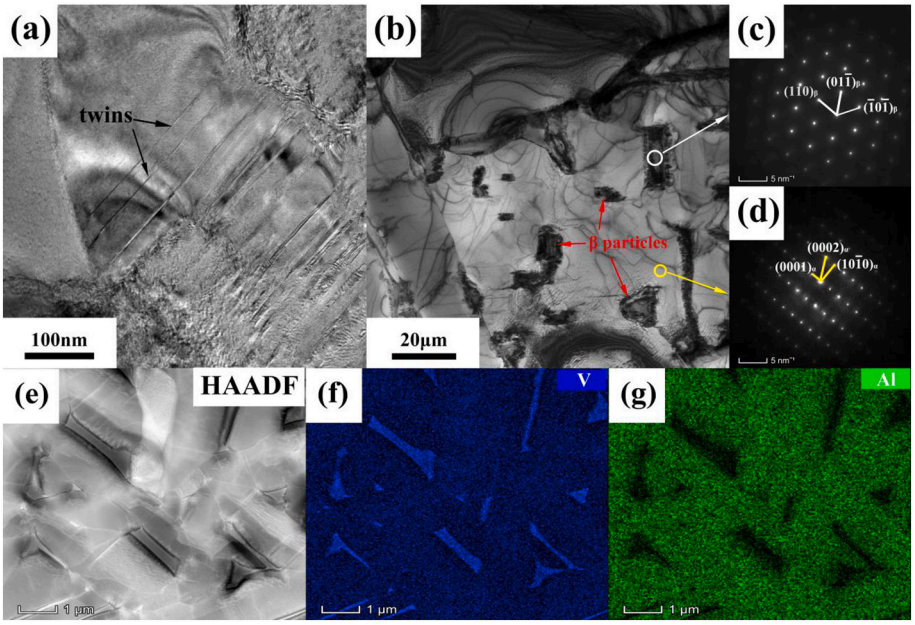

Fig. 8. TEM micrograph of the STA Ti-6Al-4V alloy: (a) Twins distributing in the matrix; (b) Fine particles β surrounded by the equiaxed α grains; (c) and (d) The corresponding selected area electron diffraction patterns of (b); (e) The EDS regions of the STA Ti-6Al-4V alloy; The corresponding EDS mapping images of (f) V element and (g) Al element.

to the ductility due to the mutual sliding of high-angle equiaxed grain boundaries. For these β dispersed phases with the size of several micrometers or even hundreds of nanometers, they can inhibit the movement of the dislocation, which will contribute to the increasing of the strength of the Ti-6Al-4V alloy. The strengthening effect is similar to the dispersion strengthening effect. Though the increasing grain size of the β matrix may cause the reduction of the strength, the strengthening effect of the fine β phases in grain interiors can make up the loss of strength and make strength larger than that of the as-fabricated Ti-6Al-4V. Therefore, the combination of the above effects can result in the higher strength and better ductility of the Ti-6Al-4V alloy.

For the formation of the special structure with the dispersed β phase surrounded by the equiaxed α phase, though it was mentioned in section 3.2, an underlying mechanism would still be described based on the results of the TEM observation. That is to say that the combined effects of the phase transformation and the element diffusion of V and Al resulted in the formation of the special microstructure. It is worth noting that the temperature and the time of STA heat treatment of the sample should be very important, which might be quite different for the as-fabricated Ti-6Al-4V samples with the various sizes and microstructures.

4. Conclusion

A novel STA heat treatment, which can simultaneously enhance the strength and ductility of the Ti-6Al-4V alloy prepared by SPS, was obtained. The effect of the heat treatment on the microstructure and mechanical properties of the Ti-6Al-4V alloy was investigated in this work. XRD, OM, SEM, and TEM were used to study the evolution of crystalline structure and microstructure of the Ti-6Al-4V alloy. The above results demonstrated that the crystalline structure of the Ti-6Al-4V alloy has no significant change by the STA heat treatment. However, after the STA heat treatment, the microstructure of Ti-6Al-4V alloy can be transformed from the Widmanstätten structure to a hierarchical structure including the basket-weave structure, the Widmanstätten structure, as well as the special microstructure, in which some fine β phases were surrounded by some equiaxed α phases. The improvement of the strength and elongation of the STA Ti-6Al-4V sample can be attributed to the comprehensive effects of annealing twins, equiaxed α, and the dispersion strengthening effect of fine β phase, respectively. This study provides a promising way to improve the overall properties of the (α + β) Ti alloy by tailoring the Widmanstätten structure with a special hierarchical structure characteristic.

Data availability

The raw/processed data required to reproduce these findings cannot be shared at this time due to legal or ethical reasons.

Declaration of Competing Interest

The authors declare that they have no known competing financial interests or personal relationships that could have appeared to influence the work reported in this paper.

Acknowledgments

This work was financially supported by the Chongqing Nature Science Foundation (Grant Nos.: 2020ZX5200033), Project funded by China Postdoctoral Science Foundation (Grant Nos.: 2020M680372) and Project funded by Chongqing Postdoctoral Science Foundation (Grant Nos.: 2021ZX5200007).

References

[1] G. Baudana, S. Biamino, D. Ugues, M. Lombardi, P. Fino, M. Pavese, C. Badini, Titanium aluminides for aerospace and automotive applications processed by Electron beam melting: contribution of Politecnico di Torino, Met. Power Rep. 71 (2016) 193–199.
[2] M.F.F.A. Hamidi, W.S.W. Harun, M. Samykano, S.A.C. Ghani, Z. Ghazalli, F. Ahmad, A.B. Sulong, A review of biocompatible metal injection molding process parameters for biomedical applications, Mater. Sci. Eng. C 78 (2017) 1263–1276.
[3] R.R. Boyer, An overview on the use of titanium in the aerospace industry, Mater. Sci. Eng. A 213 (1996) 103–114.
[4] D. Banerjee, J.C. Williams, Perspectives on titanium science and technology, Acta Mater. 61 (2013) 844–879.
[5] G. Lutjering, J.C. Williams, Titanium, Springer, 2003.
[6] G. Lutjering, Influence of processing on microstructure and mechanical properties of titanium alloys, Mater. Sci. Eng. A 243 (1998) 32–45.
[7] S. Malinov, Z. Guo, W. Sha, A. Wilson, Differential scanning calorimetry study and computer modeling of β→α phase transformation in a Ti–6Al–4V alloy, Metall. Mater. Trans. A 32 (2001) 879.
[8] Y. Chong, T. Bhattacharjee, N. Tsuji, Bi-lamellar microstructure in Ti-6Al-4V: Microstructure evolution and mechanical properties, Mater. Sci. Eng. A 762 (2019) 138077.
[9] Y. Chong, T. Bhattacharjee, J. Yi, S. Zhao, N. Tsuji, Achieving bi-lamellar microstructure with both high tensile strength and large ductility in Ti–6Al–4V alloy by novel thermomechanical processing, Materialia 8 (2019) 100479.
[10] F. Cao, K.S.R. Chandran, P. Kumar, New approach to achieve high strength powder metallurgy Ti-6Al-4V alloy through accelerated sintering at β-transus temperature and hydrogenation-dehydrogenation treatment, Scr. Mater. 130 (2017) 22–26.
[11] M.T. Jia, D.L. Zhang, B. Gabbitas, J.M. Liang, C. Kong, A novel Ti-6Al-4V alloy microstructure with very high strength and good ductility, Scr. Mater. 107 (2015) 10–13.
[12] L.M. Kang, Y.J. Cai, X.C. Luo, Z.J. Li, X.B. Liu, Z. Wang, Y.Y. Li, C. Kang, Bimorphic microstructure in Ti-6Al-4V alloy manipulated by spark plasma sintering and in-situ press forging, Scr. Mater. 193 (2021) 43–48.
[13] A. Devaraj, V.V. Joshi, A. Srivastava, S. Manandhar, V. Moxson, V.A. Duz, C. Lavender, A low-cost hierarchical nanostructured beta-titanium alloy with high strength, Nat. Commun. 8 (2017) 11176.
[14] M. Omorj, Sintering, consolidation, reaction and crystal growth by the spark plasma system (SPS), Mater. Sci. Eng. A 287 (2000) 183–188.
[15] F.J. Gil, M.P. Ginebra, J.M. Manero, J.A. Planell, Formation of α-Widmanstätten structure: effects of grain size and cooling rate on the Widmanstätten morphologies and on the mechanical properties in Ti6Al4V alloy, J. Alloys Compd. 329 (1–2) (2001) 142–152.
[16] E. Aeby-Gautier, F. Bruneseaux, J. Da Costa Teixeira, B. Appolaire, G. Geandier, S. Denis, Microstructural formation in Ti alloys: in-situ characterization of phase transformation kinetics, J. Miner. Met. Mater. Soc. 59 (2007) 54–58.
[17] M. Salib, J. Teixeira, L. Germain, E. Lamielle, N. Gey, E. Aeby-Gautier, Influence of transformation temperature on microtexture formation associated with α precipitation at β grain boundaries in a β metastable titanium alloy, Acta Mater. 61 (10) (2013) 3758–3768.
[18] A. Safdar, L.Y. Wei, A. Snis, Z. Lai, Evolution of microstructural development in electron beam melted Ti-6Al-4V, Mater. Charact. 65 (2012) 8–15.
[19] S. Fidan, E. Avcu, E. Karakulak, R. Yamanoglu, M. Zeren, T. Sinmazcelik, Effect of heat treatment on erosive wear behavior of Ti6Al4V alloy, Mater. Sci. Technol. 29 (9) (2013) 1088–1094.
[20] F.X. Gil Mur, D. Rodriguez, J.A. Planell, Influence of tempering temperature and time on the α' Ti-6Al-4V martensite, J. Alloys Compd. 234 (1996) 287–289.
[21] A. Berg, J. Kisese, L. Wagner, Microstructure gradients in Ti-3Al-8V-6Cr-4Zr-4Mo for excellent HCF strength and toughness, Mater. Sci. Eng. A 243 (1998) 146–149.
[22] S. Cao, X.G. Zhou, C.V.S. Lim, R.R. Boyer, J.C. Williams, X.H. Wu, A strong and ductile Ti-3Al-8V-6Cr-4Mo-4Zr (Beta-C) alloy achieved by introducing trace carbon addition and cold work, Scr. Mater. 178 (2020) 124–128.
[23] H.W. Deng, Z.M. Xie, B.L. Zhao, Y.K. Wang, M.M. Wang, J.F. Yang, T. Zhang, Y. Xiong, X.P. Wang, Q.F. Fang, C.S. Liu, Tailoring mechanical properties of a CoCrNi medium-entropy alloy by controlling nanotwin-HCP lamellae and annealing twins, Mater. Sci. Eng. A 744 (2019) 241–246.